and $Nb_2Br_4S_3$.[25] However, there remains the possibility that the random placement of this particular bond contributes to the amorphous nature of these materials.

One of the important conclusions reached from the systematic studies of EXAFS amplitudes was the large variability in amplitude for bridged neighbors. Accordingly, any modeling of the local structure of these materials should consider structures in which each metal has on the average more than one bridged metal neighbor. The simplest extensions are the trinuclear structures of either chainlike or cyclic form:

II III

In II the average metal-metal coordination from an EXAFS point of view would rise to $1^1/_3$, while structure III would show an average of 2 metal-metal interactions. Lengthening the former chainlike structure would raise the average metal-metal coordination asymptotically to 2. Examples of II and III such as $W_3S_9^{2-}$ and $[Mo_3S(S_2)_6]^{2-}$ are also well documented in the literature.

The dramatic spectral differences between MoS_3 and $[Mo_3S(S_2)_6]^{2-}$ rule out the presence of a significant number of triangular trinuclear clusters in MoS_3, as does the XPS data.[6] However, for the other MX_3 materials the relative distribution of dinuclear and trinuclear sites is not clear from the EXAFS and is probably better addressed by X-ray radial distribution function analysis and other studies. An important point about the trinuclear species is that they imply further reduction of the metal to provide electrons for the additional metal-metal bonds. Accordingly, for M^{4+} the stoichiometry becomes $(M^{4+})(X^{2-})(X_2^{2-})$, while for M^{3+} one could write the electronic distribution as $(M^{3+})(X_2^{2-})_{3/2}$. It is certainly possible that extensive electron delocalization makes a detailed assignment of formal oxidation states impossible and also contributes to the interesting properties of these materials.

Acknowledgment. Sue Rich and Dr. Wie-Hin Pan are thanked for their assistance in the preparation of the compounds used in this study. We also thank the staff of SSRL for their assistance in facilitating our experiments.

Registry No. MoS_3, 12033-29-3; WS_3, 12125-19-8; $MoSe_3$, 12033-30-6; WSe_3, 88981-34-4.

Supplementary Material Available: Listings of the raw EXAFS data as well as the parameterized phase shift and amplitude functions used and/or derived in this work (65 pages). Ordering information is given on any current masthead page.

(25) Drew, M. G. B.; Baba, I. B.; Rice, D. A.; Williams, D. M. *Inorg. Chim. Acta* **1980**, *44*, L217-L218.
(26) Schäfer, H.; Schäfer, G.; Weiss, A. *Z. Naturforsch., B: Anorg. Chem., Org. Chem., Biochem., Biophys., Biol.* **1964**, *19B*, 76.
(27) Dickinson, R. G.; Pauling, L. *J. Am. Chem. Soc.* **1923**, *45*, 1466.
(28) James, P. B.; Lavik, M. T. *Acta Crystallogr.* **1963**, *16*, 1183.
(29) Sasvari, K. *Acta. Crystallogr.* **1963**, *16*, 719-724.
(30) Müller, A.; Krebs, B.; Beyer, H. *Z. Naturforsch., B: Anorg. Chem., Org. Chem., Biochem., Biophys., Biol.* **1968**, *23B*, 1537-1538.
(31) Gamble, F. R. *J. Solid State Chem.* **1974**, *9*, 358-367.
(32) Müller, A.; Pohl, S.; Dartmann, M.; Cohen, J. P.; Bennett, J. M.; Kirchner, R. M. *Z. Naturforsch., B: Anorg. Chem., Org. Chem.* **1979**, *B34*, 434-436.
(33) Müller, A.; Nolte, W. O.; Krebs, B. *Angew. Chem., Int. Ed. Engl.* **1978**, *17*, 279-280.
(34) Meerschaut, A.; Rouxel, J. *J. Less-Common Met.* **1975**, *39*, 197-203, 39.

Contribution from the Laboratoire de Physicochimie des Solides, Université de Nantes, 44072 Nantes Cedex, France, and Department of Chemistry, North Carolina State University, Raleigh, North Carolina 27650

Electronic Structures of Transition-Metal Tetrachalcogenides $(MSe_4)_nI$ (M = Nb, Ta)

PASCAL GRESSIER,[1a] MYUNG-HWAN WHANGBO,*[1b,c] ALAIN MEERSCHAUT,[1a] and JEAN ROUXEL[1a]

Received July 22, 1983

Transition-metal tetraselenides $(MSe_4)_nI$ (M = Nb, Ta) contain MSe_4 chains with varying degrees of band filling. Tight-binding calculations were performed on various MSe_4 chains to probe how one-dimensional phenomena such as Peierls distortion and charge density wave formation are affected by band filling. It is found that the d_{z^2} band of an MSe_4 chain is well separated from other bands and the effect of the interchain Se···Se interaction upon the d_{z^2} band is appreciable only for those wave vectors along the chain direction $\Gamma \rightarrow Z$. The driving force for metal ion distortion along the MSe_4 chains is found to sharply diminish as the d_{z^2} band filling decreases from $^1/_2$.

In connection with low-dimensional phenomena such as Peierls distortion[2] and sliding charge density wave (CDW),[3] a new series of transition-metal tetrachalogenides $(MX_4)_nY$ (M = Nb, Ta; X = S, Se; Y = halogen) have recently been synthesized.[4] These compounds consist of MX_4 chains, which are parallel and well separated from one another by halogen atoms. This provides a pseudo-one-dimensional character to those compounds. In each MX_4 chain, a metal atom M is sandwiched by two nearly rectangular X_4 units as indicated in **1**. Any two adjacent X_4 units of **1** make a dihedral angle

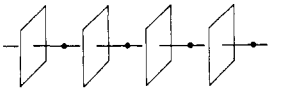

1

of almost 45°, and so a metal atom is located at the center of a rectangular antiprism of eight X atoms. For simplicity, the MX_4 chain **1** may be represented by **2**, where the heavy

2

dots refer to metal atoms M and the parallel lines perpendicular to the chain axis refer to X_4 units. **2** represents an ideal structure in which all the metal atoms are separated by the average M-M distance of *d*.

(1) (a) Université de Nantes. (b) North Carolina State University. (c) Camille and Henry Dreyfus Teacher-Scholar (1980-1985).
(2) (a) Peierls, R. E. "Quantum Theory of Solids"; Oxford University, Press: London, 1955; p 108. (b) Whangbo, M.-H. *Acc. Chem. Res.* **1983**, *16*, 95.
(3) (a) Berlinsky, A. J. *Contemp. Phys.* **1976**, *17*, 331. (b) DiSalvo, F. J. "Electron-Phonon Interactions"; Riste, T., Ed.; Plenum Press: New York, 1977; p 107. (c) White, R. M.; Geballe, T. H. "Long Range Order in Solids"; Academic Press: New York, 1979.
(4) (a) Gressier, P.; Meerschaut, A.; Guémas, L.; Rouxel, J.; Monceau, P. *J. Solid State Chem.* **1984**, *51*, 141. (b) Meerschaut, A.; Palvadeau, P.; Rouxel, J. *J. Solid State Chem.* **1977**, *20*, 21. (c) Guémas, L.; Gressier, P.; Meerschaut, A.; Louër, D.; Grandjean, D. *Rev. Chim. Miner.* **1981**, *18*, 91. (d) Gressier, P.; Guémas, L.; Meerschaut, A. *Acta Crystallogr. Sect. B: Struct. Crystallogr. Cryst. Chem.* **1982**, *38*, 2877. (e) Meerschaut, A.; Gressier, P.; Guémas, L.; Rouxel, J. *J. Solid State Chem.* **1984**, *51*, 307.

0020-1669/84/1323-1221$01.50/0

In the present work we will focus our attention on the tetraselenides $(MSe_4)_nI$ (M = Nb, Ta). In each Se_4 rectangle of the MSe_4 chains of these compounds, the shorter Se–Se side is about 2.35–2.40 Å, a distance typical of an Se_2^{2-} dimer found, for example, in $NbSe_3$.[5] The longer Se–Se side is about 3.50–3.60 Å and is comparable to the shortest interchain Se···Se separation. Thus one may regard each Se_4 rectangle as made up of two Se_2^{2-} dimers so that, if electron withdrawal by halogen atoms is neglected, each MSe_4 chain would have an M^{4+} (d^1) metal ion at the center of every Se_8 rectangular antiprism. Iodine atoms in $(MSe_4)_nI$, present between MSe_4 chains, are isolated from one another. Thus for $(MSe_4)_nI$, the average number of d electrons on each M would be $(n-1)/n$. Electronic properties of an MSe_4 chain, and hence those of $(MSe_4)_nI$ compounds, are largely determined by the interaction between metal ions along the chain axis. With the coordinate z axis taken along the chain direction, significant interaction between metal ions would occur through overlap between metal d_{z^2} orbitals. If all the metal ion d electrons are accommodated in the resulting d_{z^2} band, the extent of its band filling f is given by $f = (n-1)/2n$ for $(MSe_4)_nI$. For example, $(NbSe_4)_3I$,[4b] $(NbSe_4)_{10/3}I$,[4e] and $(TaSe_4)_2I$[4d] would have $^1/_3$-, $^7/_{20}$-, and $^1/_4$-filled d_{z^2} bands, respectively. As n increases, the d_{z^2} band of $(MSe_4)_nI$ becomes closer to $^1/_2$ filled. Vanadium tetrasulfide, VS_4, constitutes an example of the $n \rightarrow \infty$ limit, since VS_4 chains present in this compound are isostructural with **1** in essence.[6]

A linear chain with incomplete band filling (i.e., $0 < f < 1$) is susceptible to a Peierls distortion, which opens a band gap at the Fermi level. For a chain with $f \leq ^1/_2$, a Peierls distortion increases its repeat distance by a factor of $1/f$.[2,3] Thus $^1/_2$-, $^1/_3$-, and $^1/_4$-filled bands are expected to induce lattice dimerization, trimerization, and tetramerization, respectively. For example, vanadium ions of VS_4 show a dimerized structure **3** along each chain, thereby leading to short

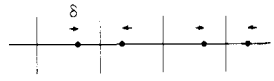

3

and long V–V bonds (i.e., 2.84 and 3.21 Å).[6] With $f = ^1/_3$, niobium ions of $(NbSe_4)_3I$ may exhibit a distorted structure, **4a** or **4b**. It is the latter that is experimentally observed.[4b]

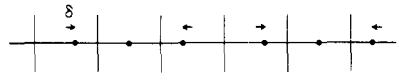

4a

4b

With $f = ^1/_4$, tantalum ions of $(TaSe_4)_2I$ are expected to show a distorted structure such as, for example, **5a** or **5b**. However, tantalum ions of each $TaSe_4$ chain are found to be equidistant at room temperature.[4d]

Upon lowering of the temperature, a metal–insulator transition occurs in $(TaSe_4)_2I$ at ~263 K.[7] A nonlinear behavior in the conductivity suggested that this phase transition

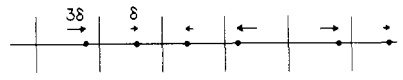

5a

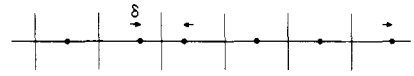

5b

is caused by an incommensurate CDW, which was later confirmed by electron diffraction.[8] A CDW refers to a periodic modulation of electron charge density distribution (precisely speaking, with respect to the electron density distribution of a metallic state, in which the periodicity of the density distribution is identical with that of the chain lattice). Thus in a CDW state, the periodicity of the density distribution is greater than that of the chain lattice. If the former is an integral multiple of the latter, the CDW involved is commensurate. Otherwise, it is incommensurate.[2,3] An incommensurate CDW arises from a partially filled band in which f is not a simple fraction of the number of lattice sites such as $^1/_2$, $^1/_3$, and $^1/_4$. Consequently, the presence of an incommensurate CDW suggests that the d_{z^2} band of $(TaSe_4)_2I$ cannot be exactly $^1/_4$ filled. As for $(NbSe_4)_{10/3}I$,[4e] a metal–insulator transition is observed at ~285 K.[9] This is associated with an incommensurate CDW. Niobium ions of $(NbSe_4)_{10/3}I$ show the distorted structure **6**, which is quite different from

6

4b observed in $(NbSe_4)_3I$ despite the similarity in their d_{z^2} band fillings (i.e., f = 0.333 and 0.350 for $(NbSe_4)_3I$ and $(NbSe_4)_{10/3}I$, respectively).

Transition-metal tetraselenides $(MSe_4)_nI$ provide MSe_4 chains with varying degrees of the d_{z^2} band filling ($0 < f < 0.5$). As discussed above, a small change in f leads to quite different structural and electrical properties. Thus, $(MSe_4)_nI$ compounds constitute an exciting series of pseudo-one-dimensional materials to study how one-dimensional phenomena such as Peierls distortion and incommensurate CDW formation are affected by band filling. To gain some insight into this question, we carried out molecular and band electronic structure calculations.

Calculations

All the $(MSe_4)_nI$ systems examined in our study are tetragonal in structure and contain two MSe_4 chains per unit cell parallel to the c axis. The shortest interchain Se···Se distance is about 3.2–3.4 Å, substantially shorter than the sum of two selenium van der Waals radii (i.e., ~4.0 Å).[10] This would give rise to some interaction between MSe_4 chains, but the shortest interchain M–M distance is ~6.7 Å while the intrachain M–M distance d is ~3.19 Å on the average. Thus the interchain Se···Se interaction, through their nearest-neighbor Se atoms, may be considered negligible as far as the essence of the d_{z^2} band is concerned. Most of our band structure calculations[11] were performed on a single MSe_4 chain for each $(MSe_4)_nI$. In order to estimate the extent of the

(5) Hodeau, J. L.; Marezio, M.; Roucau, C.; Ayroles, R.; Meerschaut, A.; Rouxel, J.; Monceau, P. *J. Phys. C* **1978**, *11*, 4117.
(6) (a) Allmann, R.; Baumann, L.; Kutoglu, A.; Rösch, H.; Hellner, E. *Naturwissenschaften* **1964**, *51*, 263. (b) Kutoglu, A.; Allmann, R. *Neues Jahrb. Mineral., Monatsh.* **1972**, *8*, 339.
(7) (a) Wang, Z. Z.; Saint-Lager, M. C.; Monceau, P.; Renard, M.; Gressier, P.; Meerschaut, A.; Guêmas, L.; Rouxel, J. *Solid State Commun.* **1983**, *46*, 325. (b) Maki, M.; Kaiser, M.; Zettle, A.; Grüner, G. *Ibid.* **1983**, *46*, 497.
(8) Roucau, C.; Ayroles, R., private communication.
(9) Wang, Z. Z.; Monceau, P.; Renard, M.; Gressier, P.; Guêmas, L.; Meerschaut, A. *Solid State Commun.* **1983**, *47*, 439.
(10) Pauling, L. "The Nature of the Chemical Bond", 3rd ed.; Cornell University Press: Ithaca, NY, 1960; p 260.
(11) (a) Whangbo, M.-H.; Hoffmann, R. *J. Am. Chem. Soc.* **1978**, *100*, 6093. (b) Whangbo, M.-H.; Hoffmann, R.; Woodward, R. B. *Proc. R. Soc. London, Ser. A* **1979**, *366*, 23.

Table I. The Exponents ζ_μ and the Valence Shell Ionization Potential $H_{\mu\mu}$ for Slater Type Atomic Orbitals χ_μ[a,b]

χ_μ	ζ_μ	ζ_μ'	$H_{\mu\mu}$, eV
Nb 5s	1.9[c]		−10.1
Nb 5p	1.85		−6.86
Nb 4d	4.08 (0.6401)	1.64 (0.5516)	−12.1
Ta 6s	2.28[c]		−10.1
Ta 6p	2.24		−6.86
Ta 5d	4.76 (0.6597)	1.94 (0.5589)	−12.1
Se 4s	2.44[d]		−20.5[e]
Se 4p	2.07		−14.4
Te 5s	2.506[d]		−20.8[e]
Te 5p	2.518		−14.8

[a] The d orbitals of Nb and Ta are given as a linear combination of two Slater type orbitals, and each is followed by the weighting coefficient in parentheses. [b] A modified Wolfsberg-Helmholz formula was used to calculate $H_{\mu\nu}$.[14] [c] Reference 15. [d] Reference 16. [e] Reference 17.

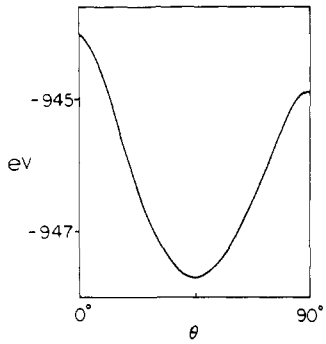

Figure 1. Total energy of $NbSe_8^{4-}$ as a function of the dihedral angle θ between the two Se_4^{4-} rectangles.

interchain Se···Se interaction, we also carried out band structure calculations on a model three-dimensional system. In the present work, the band and molecular electronic structures were calculated on the basis of the extended Hückel method.[12] The atomic parameters employed in our study are summarized in Table I.

In constructing undistorted MSe_4 chains, we employed the Se_4^{4-} rectangles of Se–Se sides 2.37 and 3.50 Å and the M–M distance of 3.19 Å. In $(MSe_4)_nI$, two adjacent Se_4^{4-} rectangles of an MSe_4 chain make a dihedral angle of ~45° (e.g., 46–50, 44–46, and 44–50° in $(NbSe_4)_3I$, $(TaSe_4)_2I$, and $(NbSe_4)_{10/3}I$, respectively). This aspect was confirmed by carrying out molecular orbital (MO) calculations on $NbSe_8^{4-}$ (**7a**) and Se_8^{8-} (**7b**) as a function of the dihedral angle θ between the two Se_4^{4-}

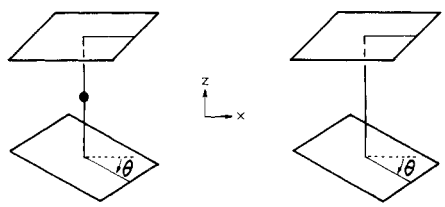

7a 7b

rectangles. The variation of the energy of $NbSe_8^{4-}$ as a function of θ is shown in Figure 1, which reveals that $NbSe_8^{4-}$ reaches the energy minimum at θ = 45° and the energy maxima at θ = 0 and 90°. A potential energy curve identical with that of Figure 1, but with a slightly less pronounced energy minimum, is also obtained for Se_8^{8-}. The energy minimum occurs at θ = 45° since the overlap between the occupied MO's of two Se_4^{4-} units is minimum at θ = 45°. This makes the destabilizing interactions between the occupied MO's minimum at θ = 45°.

(12) Hoffmann, R. *J. Chem. Phys.* **1963**, *39*, 1397.

Thus the dihedral angle θ between any two adjacent Se_4^{4-} units was taken to be 45° in our calculations. Even with this restriction, a number of relative orientations of Se_4^{4-} units are possible for MSe_4 chains. To specify such orientations, we will introduce simple notations. Shown in **8a** and **8b** are two

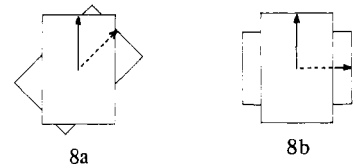

8a 8b

9a 9b

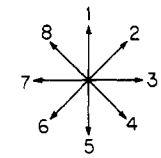

10

adjacent Se_4^{4-} units with θ = 45 and 90°, respectively, viewed along the chain direction. Let us represent each Se_4^{4-} rectangle by an arrow starting from its center to the midpoint of a short Se–Se side as shown in **8**. Then the dihedral angle between the Se_4^{4-} units in **8a** or **8b** is given by the angle between the two arrows in **9a** or **9b**, respectively. Since θ is assumed to be 45° for any two adjacent Se_4^{4-} units, the projected view of all possible orientations of the arrows along the chain is given by **10**. Note that the arrowheads of **10** are numbered successively, starting from an arbitrary position, and that the angle between any two arrows with the sequence numbers ν_i and ν_j is given by $(\nu_j - \nu_i) \times 45°$. Thus the relative arrangement of p consecutive Se_4^{4-} units may be specified by a set of p integers, $(\nu_1\nu_2\cdots\nu_p)$, where ν_i refers to the ith Se_4^{4-} unit. What matters in the specification of the relative orientation of any two Se_4^{4-} units with ν_i and ν_j is the difference $\nu_j - \nu_i$, so that ν_1 may be taken to be 1 without loss of generality. For example, in terms of the notations just described, **8a** and **8b** are represented by (12) and (13), respectively. The sequence numbers 1, 2, 3, and 4 of **10** are equivalent to 5, 6, 7, and 8, respectively. To remove possible complication resulting from this equivalence, we determine the $(\nu_1\nu_2\cdots\nu_p)$ notation such that any two consecutive numbers ν_i and ν_{i+1} are chosen to give the minimum possible difference in magnitude. According to this notation, the repeat unit cells of the MSe_4 chains in $(NbSe_4)_3I$, $(TaSe_4)_2I$, and $(NbSe_4)_{10/3}I$ are found to have the (123432), (1234), and (1234565432) arrangements of Se_4^{4-} units, respectively.[4]

Results and Discussion

d-Block Orbitals of $NbSe_8^{4-}$. The d-block levels of $NbSe_8^{4-}$ vary as a function of the dihedral angle θ as summarized in Figure 2. The symbols such as z^2 and xy indicate that the levels referred to have mainly the character of the d_{z^2} and d_{xy} orbitals, respectively. Since $NbSe_8^{4-}$ contains one Nb^{4+} (d^1) ion, the d_{z^2} level is singly occupied if $\theta \simeq 45°$. In the vicinity of θ = 45°, where the energy minimum of $NbSe_8^{4-}$ occurs, the d_{z^2} level is very well separated from the other d-block levels lying above and also from the "p-block" levels (largely Se in nature) lying below. Thus it is expected that the d_{z^2} band of an MSe_4 chain will be rather well separated out from other bands.

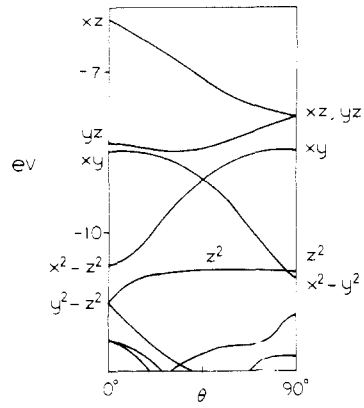

Figure 2. d-block levels of $NbSe_8^{4-}$ as a function of the dihedral angle θ between the two Se_4^{4-} rectangles.

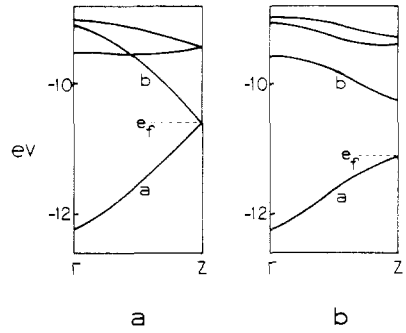

Figure 3. d-block bands of the (12)-$NbSe_4$ chain in the vicinity of the Fermi level: (a) the undistorted chain **2**; (b) the distorted chain **3** with δ = 0.1 Å.

(12)-$NbSe_4$ Chain. Because of the restriction that $\theta = 45°$, an $NbSe_4$ chain with the smallest unit cell has the (12) arrangement of Se_4^{4-} units. Such a chain may simply be termed a (12)-$NbSe_4$ chain. In general, an MSe_4 chain with the $(\nu_1\nu_2\cdots\nu_p)$ arrangement of Se_4^{4-} units can be referred to as a $(\nu_1\nu_2\cdots\nu_p)$-MSe_4 chain. As shown in Figure 3a, the d_{z^2} band of a (12)-$NbSe_4$ chain consists of two subbands (a and b). The folded structure is a consequence of the fact that there are two Nb^{4+} ions per unit cell of a (12)-$NbSe_4$ chain and that this chain has a symmetry element of glide plane. The width of the d_{z^2} band is calculated to be quite substantial (~3 eV). The top of the p-block bands, not shown in Figure 3a, lies ~0.6 eV below the bottom of band **a**. A flat band of d_{xy} and $d_{x^2-y^2}$ character overlaps slightly with band b. Thus the d_{z^2} band is rather well separated out from other bands as expected from Figure 2.

With two d electrons to fill the d_{z^2} band of Figure 3a, and band a is completely filled, hence leading to a $^1/_2$-filled d_{z^2} band. Thus the (12)-$NbSe_4$ chain would undergo a lattice dimerization **2** → **3**. The pairing distortion in **3** is defined in terms of δ, a metal ion displacement from the regular structure **2**. For a non-zero δ value, a band gap opens up at the zone edge as shown in Figure 3b. The variation of the band gap as a function of δ is shown in Figure 4. We calculated the total energy[11] of the (12)-$NbSe_4$ chain, per unit cell, as a function of δ. As summarized in Table II, this study shows that the energy minimum of (12)-$NbSe_4$ occurs at $\delta_{opt} \simeq 0.17$ Å and that **3** is more stable than **2** by 2.4 kcal/mol per $NbSe_4$ formula unit. These results on the (12)-$NbSe_4$ chain are applicable to VS_4, which consists of (1234)-VS_4 chains. Since each (1234)-VS_4 chain is isoelectronic with a (12)-$NbSe_4$ chain, it is not surprising to observe a dimerized structure such as **3** for the (1234)-VS_4 chains of VS_4.

In essence, a folded d_{z^2} band structure such as in Figure 3a originates from any (12)-MSe_4 chain. Given a $(\nu_1\nu_2\cdots\nu_p)$-MSe_4 chain, what kind of a folded d_{z^2} band should one expect? This

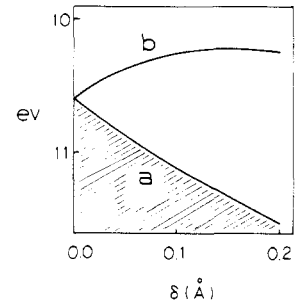

Figure 4. The top of the band a and the bottom of the band b in the (12)-$NbSe_4$ chain as a function of the **2** → **3** distortion. All the levels in the shaded region are doubly occupied.

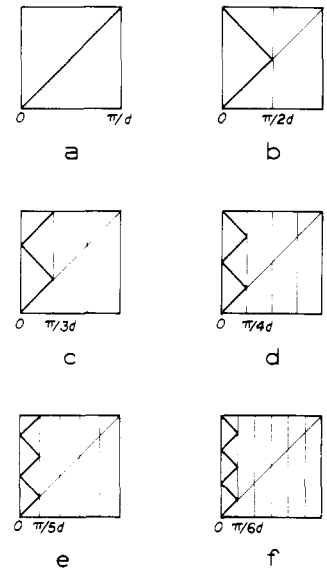

Figure 5. Effect of multipling unit cell size upon band folding. For simplicity, the band energy is assumed to be a linear function of the wave vector in (a). An increase of a unit cell size by n-fold leads to n subbands as shown in (b)–(f), where n = 2, 3, 4, 5, and 6 in (b), (c), (d), (e), and (f), respectively.

Table II. The Band Fillings f, Optimum Displacements δ_{opt}, and Relative Energies ΔE of the Distorted MSe_4 Chains **3**–**5**

chain	f	δ_{opt}, Å	ΔE,[a] kcal/mol
3	0.5	0.17	−2.4
4a	0.333	0.16	−0.6
4b	0.333	0.11	−0.4
5a	0.25	0.04	−0.2
5b	0.25	0.00	0.0

[a] Energies of the optimum distorted chains, per chain per MSe_4 formula unit, with respect to the undistorted chain **2**. A negative ΔE value means that the distorted chain is more stable than the undistorted chain.

question can be answered by considering the following problem: Suppose a chain of metal atoms in which the repeat distance is the same as the metal–metal separation d. The band structure of this chain, when calculated with one metal atom per unit cell, may be assumed to be given by Figure 5a. Without loss of generality, the band structure of this chain can also be calculated by assuming a unit cell of p consecutive metals atoms and hence a repeat distance of pd. Then such a calculation leads to a band consisting of p subbands. These are obtained by subdividing the band structure of Figure 5a into p sections of equal zone length and then folding these sections onto the first one (i.e., the one between 0 and π/pd) as illustrated in Figure 5b–f. The folded nature of the d_z^2 band of an (12)-$NbSe_4$ chain, shown in Figure 3a, is similar to that of Figure 5b. The d_{z^2} band of an undistorted (1234)-VS_4 chain

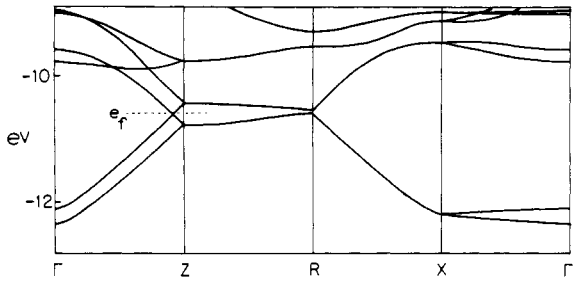

Figure 6. d-block bands of 3D-(12)-$NbSe_4$, in the vicinity of the Fermi level, along some cross sections of the Brillouin zone **12**. In fractions of the reciprocal vectors a^*, a^*, and c^*, the special points are given as Γ = (0,0,0), Z = (0,0,0.5), R = (0.5, 0, 0.5), and X = (0.5, 0, 0).

is expected to have the shape shown in Figure 5d. As already pointed out, with two d electrons per unit cell, the Fermi level of the undistorted (12)-$NbSe_4$ chain occurs at the zone edge. The Fermi level of the (1234)-VS_4 chain occurs at the zone center since there are four d electrons per unit cell. In later discussion, we will find that parts d, e, and f of Figure 5 are relevant for $(TaSe_4)_2I$, $(NbSe_4)_{10/3}I$, and $(NbSe_4)_3I$, respectively.

Interchain Se···Se Interaction. Since the shortest interchain Se···Se distance in $(MSe_4)_nI$ is substantially smaller than the sum of two selenium van der Waals radii, we need to estimate how the d-block band of a single (12)-$NbSe_4$ chain is affected by interchain Se···Se interaction. A unit cell of $(MSe_4)_nI$ contains two MSe_4 chains, so that we performed band structure calculations on a three-dimensional (3D) structure made up of (12)-$NbSe_4$ chains. In the following such a three-dimensional structure will be referred to as 3D-(12)-$NbSe_4$. **11**

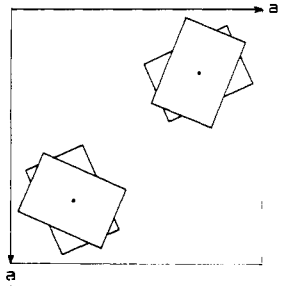

11

shows a projected view of a unit cell of 3D-(12)-$NbSe_4$ along the *c* axis, where the two (12)-$NbSe_4$ chains are arranged as found in $(TaSe_4)_2I$[4d] with the shortest interchain Se···Se distance of 3.3 Å.

Results of our band structure calculations on 3D-(12)-$NbSe_3$ are summarized in Figure 6, where Γ, Z, R, and X are special points of the Brillouin zone[13] shown in **12**. Since there are

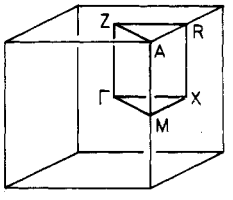

12

two (12)-$NbSe_4$ chains per unit cell, the number of d_{z^2} band

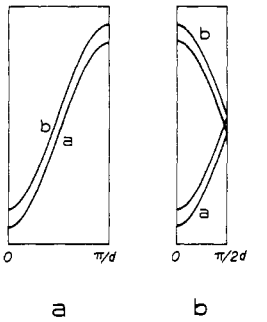

Figure 7. d_{z^2} bands along the chain direction constructed from the plane orbitals **15a** and **15b**: (a) one metal plane per unit cell; (b) two metal planes per unit cell.

levels (other band levels as well) of Figure 6 is doubled with respect to that of Figure 3a. The d_{z^2} bands of 3D-(12)-$NbSe_4$ exhibit large dispersion only along the chain direction (i.e., Γ → Z and R → X). Note that the two sets of the d_{z^2} band levels are split substantially along Γ → Z, but not at all along R → X. As far as the d_{z^2} bands are concerned, therefore, the effect of interchain interaction is significant only for those wave vectors whose values lie in the vicinity of Γ → Z. In the following we will examine why this is the case.

$(MSe_4)_nI$ compounds have planes of metal ions, sandwiched by planes of Se_2^{2-} ions, perpendicular to the MSe_4 chain axis. Thus a unit cell of $(MSe_4)_nI$, which have two MSe_4 chains, contributes two metal ions to any metal ion plane. The d_{z^2} orbitals of such metal ions lead to the bonding and antibonding combinations shown in **13a** and **13b**, respectively. For sim-

13a **13b**

14a **14b**

plicity, **13a** and **13b** may be represented by the projected views onto the metal ion plane **14a** and **14b**, respectively. For wave vectors along Γ → Z, $k_x = k_y = 0$. Therefore, the metal ions of a given plane are described by the "plane orbitals" arising from **14a** and **14b**. One plane orbital **15a** is obtained by

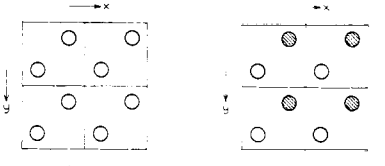

15a **15b**

repeating **14a** along the two interchain directions without any sign change. The other plane orbital **15b** results from **14b** in a similar manner. It is evident that **15a** is more stable than **15b**. The plane orbitals **15a** and **15b** are present in each metal ion plane, and they interact along the chain axis to form two d_{z^2} bands such as illustrated in Figure 7a. Here the d_{z^2} bands a and b result from **15a** and **15b**, respectively. For **11**, which consists of (12)-$NbSe_4$ chains, there are two metal ion planes per unit cell so that the folding procedure described in Figure 5b leads to the d_{z^2} bands of Figure 7b for **11**. Along X → R, wave vectors are such that $k_x = \pi/a$ and $k_y = 0$, where *a* is the repeat distance along the interchain direction. Thus the plane orbitals resulting from **14a** and **14b** are given by **16a**

(13) Lax, M. "Symmetry Principles in Solid State and Molecular Physics"; Wiley: New York, 1974.
(14) Ammeter, J. H.; Bürgi, H.-B.; Thibeault, J. C.; Hoffmann, R. *J. Am. Chem. Soc.* **1978**, *100*, 3686.
(15) Basch, H.; Gray, H. B. *Theor. Chim. Acta* **1966**, *4*, 367.
(16) Clementi, E.; Roetti, C. *At. Data Nucl. Data Tables* **1974**, *14*, 179.
(17) Hinze, J.; Jaffé, H. H. *J. Phys. Chem.* **1963**, *67*, 1501.

and **16b**, respectively. That is, unit cell patterns alternate their

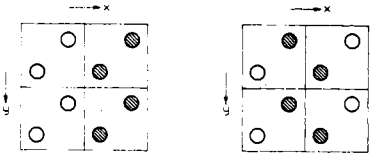

16a 16b

signs only along the x direction. Due to the translational symmetry, **16a** and **16b** are degenerate and give rise to the degeneracy of the d_{z^2} bands in Figure 6 along X → R. Along M → A of the Brillouin zone (see **12**) in which $k_x = k_y = \pi/a$, the two plane orbitals arising from **14a** and **14b** are given by **17a** and **17b**, respectively. These two plane orbitals are again

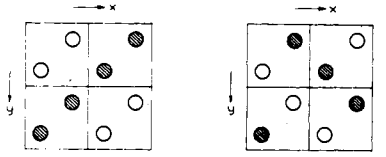

17a 17b

degenerate so that the d_{z^2} bands along M → A, though not shown in Figure 6, would be degenerate. Consequently, the extent of the d_{z^2} band splitting, which reflects the magnitude of the interchain Se···Se interaction, is significant only along Γ → Z. The present band structure calculations on 3D-(12)-$NbSe_4$ show that the width of the d_{z^2} band along the chain direction is about 3 eV while that along the interchain direction is about 0.25 eV.

The above discussion reveals that, as far as the d_{z^2} bands are concerned, the effect of the interchain interaction is small in magnitude and can be seen only along Γ → Z. In the remainder of this work, therefore, our discussion on $(MSe_4)_nI$ will be based upon calculations on single MSe_4 chains. As shown in Figure 8, the effect of the interchain Se···Se interaction can be incorporated into our discussion by simply doubling the d_{z^2} bands along Γ → Z of single-chain calculations with a separation of ~0.25 eV.

$(NbSe_4)_3I$. Along each $NbSe_4$ chain of $(NbSe_4)_3I$, niobium ions are found to have the distorted structure **4b** with $\delta \simeq 0.06$ Å.[4b] Due to the requirement that the dihedral angle θ between adjacent Se_4^{4-} units is ~45° in an $NbSe_4$ chain, the minimum number of Se_4^{4-} units needed to repeat with the niobium ion distortion of **4b** is 6 as found from the (123432)-$NbSe_4$ chains of $(NbSe_4)_3I$. It is those niobium ions present on both sides of the Se_4^{4-} rectangle 1 and 4 that are involved in the pairing of **4b**. Such niobium ions are enclosed by two Se_4^{4-} rectangles arranged eclipsed to each other.

The d_{z^2} band structure of a (123432)-$NbSe_4$ chain is expected to exhibit six subbands as illustrated in Figure 5f. The bottom four subbands of a (123432)-$NbSe_4$ chain with equidistant separation of niobium ions are shown in Figure 9. Unlike in Figure 5f, there exists a small gap between the bands b and c in Figure 9. This is due to lack of a screw rotation symmetry for the (123432)-$NbSe_4$ chain. Since there are four d electrons per unit cell, the bands a and b are completely filled. For interactions between niobium ions along the chain axis, d_{z^2} orbitals are topologically similar to s orbitals. To simplify our diagrams, therefore, we may represent d_{z^2} orbitals by s orbitals. Then the top of band b and the bottom of band c have the nodal properties shown in **18a** and **18b**, respectively.

18a

18b

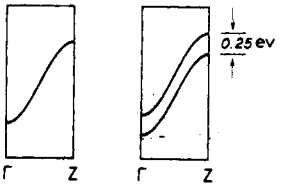

a b

Figure 8. Effect of the interchain Se···Se interaction upon band structure: (a) hypothetical band of a single MSe_4 chain; (b) band structure expected for the three-dimensional crystal constructed from a unit cell containing two MSe_4 chains.

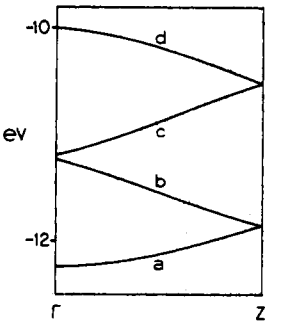

Figure 9. The bottom four of the six d_{z^2} subbands calculated for a (123432)-$NbSe_4$ chain.

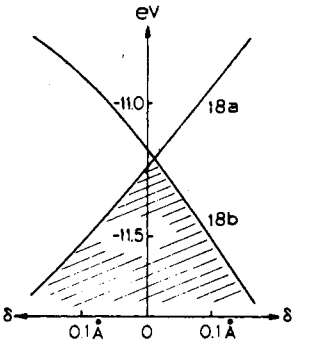

Figure 10. Variation of the band levels **18a** and **18b** as a function of the distortions **2** → **4a** and **2** → **4b**. All the levels in the shaded region are doubly occupied.

In terms of band structure calculations, the distortions **2** → **4a** and **2** → **4c** were also examined for the (123432)-$NbSe_4$ chain as a function of δ. The essential feature of the d_{z^2} band structure of **4a** or **4b** is similar to that shown in Figure 9. The band level **18a** is stabilized by the **2′** → **4b** distortion but destabilized by the **2** → **4a** distortion, while the opposite is the case for the band level **18b**. This is summarized in Figure 10, which shows that, in the distorted structure **4a**, the band levels **18a** and **18b** become the bottom of the d_{z^2} band c and the top of the d_{z^2} band b, respectively. In any event, the band gap of the (123432)-$NbSe_4$ chain is given by the energy difference between the band levels **18a** and **18b**. From the total energy values per unit cell[11] calculated as a function of δ, summarized in Table II, we obtain the following results: (a) The optimum structure of **4a** occurs at $\delta_{opt} \simeq 0.16$ Å and that of **4b** at $\delta^{opt} \simeq 0.11$ Å. (b) The optimum structures of **4a** and **4b** are both more stable than the undistorted structure **2**. However, the stability difference between **4a** and **4b** is very small. (c) The band gaps of **4a** and **4b** at their optimum structures are 0.63 and 0.95 eV, respectively. This provides a semiconducting property for $(NbSe_4)_3I$.[4a]

$(TaSe_4)_2I$. $(TaSe_4)_2I$ consists of (1234)-$TaSe_4$ chains,[4d] which show no metal atom distortion in contrast to the (123432)-$NbSe_4$ chains of $(NbSe_4)_3I$. It is important to gain

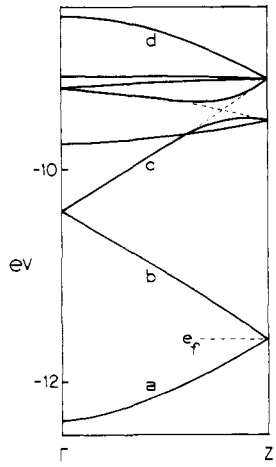

Figure 11. d_{z^2} band structure of the (1234)-$TaSe_4$ chain.

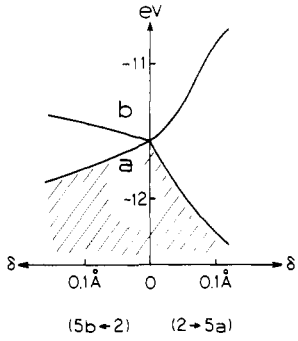

Figure 12. Band gap of the (1234)-$TaSe_4$ chain as a function of the distortions **2** → **5a** and **2** → **5b**. All the levels in the shaded region are doubly occupied.

some insight into why the (1234)-$TaSe_4$ chains exhibit no distortion and whether or not this is related to the occurrence of an incommensurate CDW in $(TaSe_4)_2I$.[7] Figure 11 shows the d_{z^2} band structure of a (1234)-$TaSe_4$ chain with equidistant metal ion separation. The four subbands as expected from Figure 5d correspond to the bands a–d of Figure 11.

The bands a, b, and d have d_{z^2} character throughout the zone. The band c has d_{z^2} character near the zone center but d_{xy} and $d_{x^2-y^2}$ character at the zone edge. This is due to the fact that two bands having d_{xy} and $d_{x^2-y^2}$ character overlap with band c, as indicated by the dashed lines in Figure 11. With two d electrons per unit cell, only the band a is completely filled, thereby leading to the Fermi level at the zone edge. Therefore, if the presence of the four bands of d_{xy} and $d_{x^2-y^2}$ character is neglected, the d_{z^2} orbital of a (1234)-$TaSe_4$ chain is $^1/_4$ filled.

Upon the **2** → **5a** or **2** → **5b** distortion, a band gap opens up at the zone edge. Figure 12 shows how the band gap between bands a and b increases by the **2** → **5a** and **2** → **5b** distortions. The total energies of **5a** and **5b** per unit cell calculated as a function of δ are summarized in Table II. This show that very little energy is gained by the distortion **2** → **5a**, and further there is no energy gain for the **2** → **5b** distortion. It is important to observe from Table II that the driving force toward distortion is greatest for a $^1/_2$-filled chain and diminishes sharply as the band filling f decreases from $^1/_2$. This is consistent with why no permanent distortion is observed for the (1234)-$TaSe_4$ chains of $(TaSe_4)_2I$.

As discussed in terms of Figure 8, the effect of the interchain Se···Se interaction can be incorporated into our discussion by simply doubling the d_{z^2} band structure of a single chain with a separation of ~0.25 eV. According to this prescription, the d_{z^2} band structure of 3D-(1234)-$TaSe_4$ may be given as shown in Figure 13b in the vicnity of the Fermi level. According to

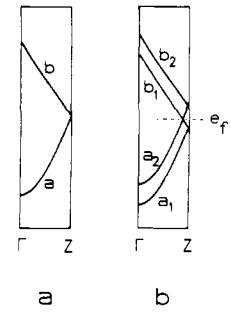

Figure 13. Effect of the interchain Se···Se interaction on the d_{z^2} band structure of $(TaSe_4)_2I$: (a) bottom two subbands of the (1234)-$TaSe_4$ chain (see Figure 11); (b) corresponding band structure expected for 3D-(1234)-$TaSe_4$.

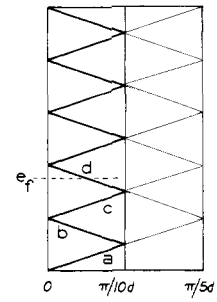

Figure 14. d_{z^2} band folding expected for a (1234565432)-$NbSe_4$ chain.

15a and **15b** the two overlapping bands of Figure 13b have different symmetry properties so that they cross each other. This leads to the Fermi wave vector of $k_f \simeq 0.44\ c^*$ for 3D-(1234)-$TaSe_4$, where $c^* = 2\pi/c$ with the repeat distance c ($=4d$) along the chain direction. This is in reasonable agreement with the CDW vector $2k_f = 16c^*/17$ ($\simeq 0.94c^*$) recently observed by electron diffraction.[8]

$(NbSe_4)_{10/3}I$. $(NbSe_4)_{10/3}I$ consists of (1234565432)-$NbSe_4$ chains.[4e] These chains exhibit the metal ion distortion shown in **6** ($\delta \simeq \delta' \simeq 0.02$ Å). One can observe the components of **2** → **4a** and **2** → **4b** distortions from **6**. It is surprising that a small difference in the band filling (i.e., $f = 0.333$ and 0.350 for the (123432)-$NbSe_4$ and (1234565432)-$NbSe_4$ chains, respectively) could lead to such a delicate change in the distortion pattern.

The unit cell of a (1234565432)-$NbSe_4$ chain is large so that actual band calculations on the chain were not performed. Nevertheless, the d_{z^2} band structure of an undistorted (1234565432)-$NbSe_4$ chain can be derived from Figure 5e. Since a (1234565432)-$NbSe_4$ chain contains 10 metal ions per unit cell, its d_{z^2} band structure will have 10 subbands as depicted in Figure 14. This is obtained by folding the right half of the band in Figure 5e onto its left half. With seven d electrons per unit cell, the three bands a–c of Figure 14 are completely filled while the fourth band d becomes $^1/_2$ filled. This leads to the Fermi wave vector $k_f = c^*/4$, where $c = 10d$. This feature is expected to remain so even if the **2** → **6** distortion is present in the (1234565432)-$NbSe_4$ chain, since the distortion does not open up a band gap in the middle of any subband of Figure 14. This aspect plus the interchain Se···Se interaction effect may be responsible for the observation that $(NbSe_4)_{10/3}I$ exhibits an incommensurate CDW despite the presence of the distortion **6** in the chains.[9]

Concluding Remarks

$(MSe_4)_nI$ compounds contain MSe_4 chains with varying degrees of d_{z^2} band filling. The distortion pattern of the metal ions in the MSe_4 chains depends critically upon the band filling, and so does the electrical conductivity of $(MSe_4)_nI$. Our band structure study shows that the d_{z^2} band of an MSe_4 chain is well separated out from other bands. This is due to the

requirement that the dihedral angle betweeen any two adjacent Se_4^{4-} rectangles be ~45°. The effect of the interchain Se···Se interaction upon the d_{z^2} band structure is found to be appreciable only for those wave vectors along the chain direction (i.e., $\Gamma \rightarrow Z$), which provides a pseudo-one-dimensionality to $(MSe_4)_nI$. Our study also shows that the driving force for the metal ion distortion in the MSe_4 chains diminishes sharply as the d_{z^2} band filling f decreases from $^1/_2$. This is understandable, since the d_{z^2} band orbital at the Fermi level becomes less noded (i.e., more bonding between metal ions) as $f = {}^1/_2 \rightarrow 0$. The apparent absence of a permanent metal ion distortion and the presence of an incommensurate CDW in $(TaSe_4)_2I$ seem to reflect the low band filling (i.e., $f = {}^1/_4$) and the interchain Se···Se interaction.

According to the present study, the **2** → **4a** distortion is as probable as the **2** → **4b** distortion in $(NbSe_4)_3I$. In terms of the lattice strain, the former is expected to be less preferred. Nevertheless, one cannot discount the possibility that the **2** → **4a** distortion can be an alternative to **2** → **4b** at low temperature. For the (1234)-$TaSe_4$ chain, the **2** → **5a** distortion is calculated to have some energy lowering effect. But this distortion is expected to exert significant lattice strain.

Acknowledgment. This work was in part supported by the Camille and Henry Dreyfus Foundation through a Teacher-Scholar Award to M.-H.W., which made it possible for P.G. to visit North Carolina State University. M.-H.W. is grateful to Professor J. K. Burdett for valuable discussion and to Dr. F. J. DiSalvo for information concerning $(MX_4)_nY$ compounds.

Note Added in Proof. A recent X-ray diffraction study of Fujishita et al.[18] on $(MSe_4)_2I$ (M = Nb, Ta) shows that the CDW vector, $2k_f$, along the chain direction is $0.085c^*$, which is equivalent to $0.915c^*$. Our estimate of $2k_f = 0.88c^*$ is in good agreement with this observation.

Registry No. $NbSe_4$, 12034-79-6; $TaSe_4$, 79730-35-1.

(18) Fujishita, H.; Sato, M.; Hoshino, S. *Solid State Commun.* **1984**, *49*, 313.

Contribution from the Department of Chemistry, North Carolina State University, Raleigh, North Carolina 27650, and Laboratoire de Physicochimie des Solides, Université de Nantes, 44072 Nantes Cedex, France

Band Structure of $NbTe_4$

MYUNG-HWAN WHANGBO*[1a,c] and PASCAL GRESSIER[1b]

Received July 22, 1983

Transition-metal tetratelluride chains MTe_4 (M = Nb, Ta) adopt a structure different from that of other tetrachalcogenide chains. Tight-binding calculations on $NbTe_4$ show that multidimensional character is substantially stronger in $NbTe_4$ than in $(MSe_4)_nI$. The $^1/_2$-filled d_{z^2} band of $NbTe_4$ leads to a Fermi surface with two nearly flat pieces, which gives rise to three charge density wave nesting vectors. The band electronic structure of $NbTe_4$ is consistent with the view that in $NbTe_4$ each metal ion Nb^{4+} (d^1) is surrounded by eight Te_2^{2-} dimers.

Chains of general formula MX_4 (M = V, Nb, Ta; X = S, Se, Te) are present in ternary compounds $(MX_4)_nY$ (Y = halogen) and in binary compounds MX_4. These MX_4 chains are found to exhibit two different structures. In the tetraselenides $(MSe_4)_nI$ (M = Nb, Ta),[2] MSe_4 chains are parallel and well separated from one another by iodine atoms. Each metal atom M of an MSe_4 chain is located at the center of an antiprism made up of two *rectangular* Se_4 units as shown in **1**, where the dihedral angle between two adjacent Se_4 units

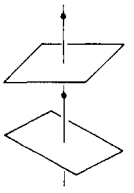

1

is close to 45°. The view of two neighboring Se_4 units projected along the chain axis is shown in **2**. In each Se_4 unit, the

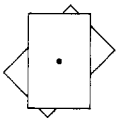

2

shorter Se–Se side (2.35–2.40 Å) is very close to the Se–Se distance of an Se_2^{2-} dimer,[2a,3] while the longer Se–Se side is close to the shortest interchain Se···Se separation. Therefore, each Se_4 rectangle can be considered as made up of two Se_2^{2-} dimers. Thus, if electron removal of iodine atoms is neglected, an MSe_4 chain of $(MSe_4)_nI$ contains an M^{4+} (d^1) ion at the center of every rectangular antiprism of selenium.[2a]

The VS_4 chains present in the binary compound VS_4[4] are found to be isostructural with the MSe_4 chains of $(MSe_4)_nI$. However, this is not the case for the MTe_4 chains of binary compounds MTe_4 (M = Nb, Ta).[5] As shown in the projected view **3a** along the *c* axis, each metal atom of MTe_4 is now located at the center of an antiprism made up of two *square* Te_4 units. It is interesting to consider the formal oxidation state of a metal atom in MTe_4. If each tellurium were to exist as Te^{2-}, there would be no electrons in the d-block bands of MTe_4 and the top portion of the tellurium p-block band should

(1) (a) North Carolina State University. (b) Université de Nantes. (c) Camille and Henry Dreyfus Teacher-Scholar (1980–1985).

(2) (a) Gressier, P.; Whangbo, M.-H.; Meerschaut, A.; Rouxel, J. *Inorg. Chem.*, preceding paper in this issue. (b) Gressier, P.; Meerschaut, A.; Guémas, L.; Rouxel, J.; Monceau, P. *J. Solid State Chem.* **1984**, *51*, 141. (c) Meerschaut, A.; Palvadeau, P.; Rouxel, J. *Ibid.* **1977**, *20*, 21. (d) Guémas, L.; Gressier, P.; Meerschaut, A.; Louer, D.; Grandjean, D. *Rev. Chim. Miner.* **1981**, *18*, 91. (e) Gressier, P.; Guémas, L.; Meerschaut, A. *Acta Crystallogr., Sect. B: Struct. Crystallogr. Cryst. Chem.* **1982**, *38*, 2877. (f) Meerschaut, A.; Gressier, P.; Guémas, L.; Rouxel, J. *J. Solid State Chem.*, in press.

(3) Hodeau, J. L.; Marezio, M.; Roucau, C.; Ayroles, R.; Meerschaut, A.; Rouxel, J.; Monceau, P. *J. Phys. C* **1978**, *11*, 4117.

(4) (a) Allmann, R.; Baumann, L.; Kutoglu, A.; Rösch, H.; Hellner, E. *Naturwissenschaften* **1964**, *51*, 263. (b) Kutoglu, A.; Allmann, R. *Neues Jahrb. Mineral. Monatsh.* **1972**, *8*, 339.

(5) (a) Selte, K.; Kjekshus, A. *Acta Chem. Scand.* **1964**, *18*, 690. (b) Bjerkelund, E.; Kjekshus, A. *J. Less-Common Met.* **1964**, *7*, 231.

0020-1669/84/1323-1228$01.50/0